Energy Economics 149 (2025) 108737

Contents lists available at ScienceDirect

Energy Economics

journal homepage: www.elsevier.com/locate/eneeco

Pricing energy futures options: The role of seasonality and liquidity

Wenting Chen [a], Zhao Yang [b], Xin-Jiang He [c,d,*]

[a] Department of Business, Jiangnan University, Wuxi, Jiangsu, China
[b] School of Mathematics and Applied Statistics, University of Wollongong, Wollongong, NSW, Australia
[c] School of Economics, Zhejiang University of Technology, Hangzhou, China
[d] Institute for Industrial System Modernization, Zhejiang University of Technology, Hangzhou, China

ARTICLE INFO

JEL classification:
G13
C02
G17
Q47
C61
C63

Keywords:
Energy futures option
Seasonality
Liquidity risk
Option pricing

ABSTRACT

In this paper, we propose an enhanced pricing framework for energy derivatives by incorporating seasonal effects and liquidity risks into the traditional two-factor model. The main theoretical challenge lies in deriving a tractable semi-analytical solution for the price of energy futures options under this enhanced model specification, which we have successfully achieved through advanced analytical techniques. Our solution demonstrates superior computational efficiency compared to the Monte-Carlo method, and greatly facilitates the model calibration process. Empirical results reveal that the proposed model outperforms both the standard two-factor model and the model with a seasonal-only specification, validating the importance of jointly modeling seasonal factors and liquidity risks for pricing energy futures options.

1. Introduction

Nowadays, energy futures options have become increasingly important in global financial markets. According to Bank for International Settlements (BIS, 2023), energy derivatives constituted 64% of all commodity derivatives by notional value in 2023, with crude oil and natural gas contracts alone accounting for 82% of energy derivatives trading volume on major exchanges (CME Group, 2023). While traditional pricing models (Gibson and Schwartz, 1990; Schwartz, 1997; Schwartz and Smith, 2000) established foundational frameworks using convenience yield and cost-of-carry concepts, they often inadequately address energy markets' distinctive features, particularly the noticeable seasonal patterns (e.g., winter heating demand cycles) and stochastic liquidity conditions. These oversimplifications frequently result in significant pricing inaccuracies during seasonal transitions or market stress periods, highlighting the need for more sophisticated models to account for energy derivatives' unique characteristics.

Seasonality is one of the fundamental drivers of the price dynamics in energy markets, where predictable fluctuations emerge from cyclical demand patterns and supply constraints. Unlike agricultural commodities, whose seasonality stems mainly from production cycles, energy commodities usually exhibit sharp seasonal volatility spikes tied to weather-sensitive demand (Chen et al., 2022; Ewald et al., 2022). These patterns are so pronounced that conventional pricing models which ignore seasonal effects routinely misprice energy derivatives, particularly those with expirations aligned with demand peaks (Mellios et al., 2016). Recent advances demonstrate the importance of explicitly modeling seasonality in the pricing of energy derivatives. For instance, Constant et al. (2023) showed that seasonal jump–diffusion models reduce pricing errors in WTI crude options significantly during transitional months. Similarly, Frau and Fanelli (2024) proved that dual-component seasonal volatility captures 92% of observed price variance in European gas options. These findings confirm that seasonality is not merely a statistical refinement but a first-order determinant of energy option valuation, whose omission will generate significant errors in the calculations for the Greeks.

Liquidity risk is another critical but often neglected factor in the pricing of energy derivatives. Recent studies demonstrate that energy derivatives are particularly sensitive to liquidity fluctuations due to their unique market microstructure, where geopolitical disruptions and physical delivery constraints frequently trigger abrupt liquidity dry-ups (Kalaitzoglou and Ibrahim, 2015). Zhang and Ding (2018) found that liquidity shocks account for nearly 30% of volatility in crude oil options markets, while Hu et al. (2020) revealed how liquidity constraints amplify cross-market contagion during periods of stress, particularly between energy and equity markets. Research conducted

* Corresponding author at: School of Economics, Zhejiang University of Technology, Hangzhou, China.
E-mail addresses: wtchen@jiangnan.edu.cn (W. Chen), zy686@uowmail.edu.au (Z. Yang), xinjiang@zjut.edu.cn (X.-J. He).

https://doi.org/10.1016/j.eneco.2025.108737
Received 10 May 2025; Accepted 11 July 2025
Available online 30 July 2025

by Jain et al. (2024), Okoroafor and Leirvik (2024), Peng et al. (2024) and their references provides more insights into the function of liquidity in commodity markets. Despite these advances, quantitative research examining how liquidity risks affect the price of futures options remains limited, with particularly sparse evidence for energy-related contracts. The best methods for modeling financial derivatives with liquidity risks are still debated (Leippold and Schärer, 2017; Liu and Yong, 2005; Loeper, 2018). Recently, the methodology of considering market liquidity as an overarching variable and adjusting individual stock prices appropriately has gained the most attention (Feng et al., 2014), particularly in the context of derivatives pricing (Li et al., 2018; Pasricha et al., 2022; Lin et al., 2025; He et al., 2025b).

Indeed, seasonality and liquidity risks represent two prevalent factors in energy markets. However, their application to energy derivatives has been insufficiently explored. This study contributes to the literature by proposing a new pricing framework that simultaneously incorporates deterministic seasonal patterns and stochastic liquidity dynamics. The primary theoretical advancement lies in deriving a semi-closed-form analytical solution for commodity futures options, overcoming mathematical challenges posed by the nonlinear interaction of these factors. Compared to the Monte-Carlo (MC) simulations, our analytical approach demonstrates superior computational efficiency. The model's practical utility is further confirmed through an empirical investigation using INE crude oil options data. By successfully integrating these critical yet previously overlooked market characteristics into a tractable pricing framework, this work provides market participants with a more reliable tool for the valuation of energy derivatives, particularly during periods of seasonal transition and/or liquidity stress.

The subsequent sections of the paper are organized as follows. Section 2 presents the return dynamics in details. Section 3 outlines the derivation of the analytical pricing formula for commodity futures options. Section 4 numerically validates the pricing formula and presents several discussions. Section 5 analyzes empirically the applicability of the newly proposed model to the energy market. Concluding remarks are given in the last section.

2. Return dynamics

This section presents the return dynamics of commodity prices influenced by seasonal factors and liquidity risks. The return dynamics of commodity prices is defined on a complete probability space (Ω, F, P) within a finite time horizon $[t, T^*]$, where P is the physical measure, $T^* < \infty$, and t is the current time. All the stochastic processes described below are assumed to be $\{F_t\}_{t\geq 0}$-adapted. It is also assumed that commodities exhibit imperfect liquidity, which occurs in conditions of market surplus or short supply. Note that the results of this section, along with those in the next two sections, apply generally to commodity derivatives, including but not limited to energy markets.

Denote the market commodity price at t as S_t. Note that this price is observable, and affected by both seasonality and liquidity risks. To separate the impacts of liquidity risks, we introduce S_t^* as the potential commodity price without the impact of liquidity risks. Following Ma et al. (2020), we assume that S_t^* satisfies the following two-factor model with seasonality:

$$\begin{aligned} dS_t^* &= (\mu - y_t)S_t^* dt + \sigma_1 S_t^* \mathrm{d}W_{1,t}^P, \\ dy_t &= \kappa_y[\theta(t) - y_t]dt + \sigma_y e^{\psi(t)} dW_{2,t}^P, \end{aligned} \tag{2.1}$$

where y_t represents the convenience yield; $\kappa_y > 0$ and $\theta(t) > 0$ are the mean-reversion rate and long-term mean of y_t, respectively; $\sigma_1 \geq 0$ and $\sigma_y \geq 0$ are the volatilities of S_t^* and y_t, respectively. Moreover, the convenience yield and the potential commodity price are correlated with $\rho_{zy} \in [-1, 1]$. $\phi(t)$ and $\theta(t)$ denote the seasonal impact and are defined as

$$\psi(t) = q\sin(2\pi(t+\upsilon))$$

$$\theta(t) = \theta_0 + \sum_{n=1}^{N}[\gamma_n \cos(2\pi nt) + \gamma_n^* \sin(2\pi nt)],$$

respectively. Here, $q \geq 0$ is a constant, and $\upsilon \in [-0.5, 0.5]$ ensures parameter uniqueness. The 1st of January serves as the time origin. In addition, θ_0, γ_n and γ_n^* are constants. N represents the number of trigonometric coefficients, and is usually set to 2 (Ewald and Ouyang, 2017; Ma et al., 2020).

It should be remarked that (2.1) relates to various established models for commodity derivatives in the existing literature. In the absence of time-varying volatility (i.e., $\psi(t) = 0$), (2.1) is identical to the model proposed by Ewald and Ouyang (2017). Additionally, in the absence of seasonality and with constant return volatility, as indicated by $\psi(t)$, γ_n, and γ_n^* all equal to zero, (2.1) degenerates to the one proposed by Schwartz (1997).

We also remark that the trigonometric specifications of $\theta(t)$ and $\psi(t)$ can effectively capture the dual seasonal patterns of energy markets: price levels (e.g., higher winter/summer electricity demand) and volatility dynamics (e.g., supply shocks during extreme weather), capturing how cyclical factors systematically influence both trends and market fluctuations. The Fourier-based $\theta(t)$ component models the recurring price patterns observed in energy commodities through smooth periodic functions, accurately reflecting seasonal variations in convenience yields driven by heating demand and refinery cycles (Geman, 2005). Simultaneously, $\psi(t)$ accounts for the well-documented volatility clustering during critical periods such as winter demand peaks and hurricane seasons. This integrated formulation provides a mathematically tractable yet realistic representation of the seasonality observed in energy markets, maintaining consistency with observed price and volatility dynamics across different trading horizons (Lucia and Schwartz, 2002) while avoiding the oversimplifications of conventional single-factor models.

After considering the seasonal factors, we now take the liquidity risks into consideration. Following Feng et al. (2014), we further assume that the market price and the potential commodity price are related through $S_t = \frac{S_t^*}{\zeta_t}$, where ζ_t is the liquidity discount factor and satisfies $\frac{d\zeta_t}{\zeta_t} = (\frac{1}{2}\xi^2 l_t^2 - \xi l_t)dt - \xi l_t dW_{3,t}^P$. Here, $\xi > 0$ is the sensitivity of the commodity price to the level of market illiquidity, l_t is the liquidity risk level of the market, and $W_{3,t}^P$ is a Brownian motion that is independent with respect to (w.r.t) both $W_{1,t}^P$ and $W_{2,t}^P$. According to Itô's lemma, we have

$$\frac{dS_t}{S_t} = (\mu - y_t + \xi l_t + \frac{1}{2}\xi^2 l_t^2)dt + \sigma_1 dW_{1,t}^P + \xi l_t dW_{3,t}^P.$$

Furthermore, the liquidity l_t is assumed to follow

$$dl_t = \alpha(\beta - l_t)dt + \eta dW_{4,t}^P,$$

where $\mathrm{cov}(dW_{4,t}^P, dW_{1,t}^P) = 0$, $\mathrm{cov}(dW_{4,t}^P, dW_{2,t}^P) = 0$, and $\mathrm{cov}(dW_{4,t}^P, dW_{3,t}^P) = \rho_{\zeta l}dt$. Note that the liquidity discount factor ζ_t is related to both mean-reversion stochastic market liquidity and the sensitivity of commodity prices to market illiquidity.

To demonstrate our work in a clear manner, in the following, we refer to the model with stochastic convenience yield and seasonal factors as the CS model, and the newly proposed model as CSL model. We also denote several filtrations before the solution procedure is presented. Let F^S, F^y and F^l be the filtrations generated by S_t, y_t and l_t, respectively. These filtrations are all assumed to be right continuous and P-complete. We additionally define an enlarged filtration $\{g(t) := F^G(t) | t \in [0, T^*]\}$ where $F^G(t) := F^S(t) \vee F^y(t) \vee F^l(t)$. Here, $A \vee B$ denotes the minimal σ-field containing the σ-fields of both A and B.

3. Solution procedure

This section investigates the pricing of futures options within the framework of the newly proposed CSL model. This section is divided into three subsections, according to three important issues to be addressed. In the first subsection, an appropriate equivalent martingale measure is identified. In the second subsection, the derivation of the analytical expression for the futures price is presented, based on which, the analytical price for the futures options is derived in the third subsection.

3.1. An equivalent martingale measure

When a market is not perfectly liquid, it is incomplete. Many equivalent martingale measures can be adopted to price contingent claims in such an incomplete market. A certain principle should thus be employed to identify an equivalent comparable martingale measure.

The dynamics of the commodity price need to be firstly rewritten to clearly reflect the correlated structure of the involved Brownian motions. Specifically, we rewrite the dynamics of S_t as

$$\frac{dS_t}{S_t} = (\mu - y_t + \xi l_t + \frac{1}{2}\xi^2 l_t^2)dt + \sigma_1(\rho_{zy}dW_{2,t}^P + \sqrt{1-\rho_{zy}^2}d\bar{W}_{2,t}^P) + \xi l_t(\rho_{\zeta l}dW_{4,t}^P + \sqrt{1-\rho_{\zeta l}^2}d\bar{W}_{4,t}^P),$$

where $W_{2,t}^P$, $\bar{W}_{2,t}^P$, $W_{4,t}^P$, and $\bar{W}_{4,t}^P$ are independent with each other.

Now, link a risk-neutral measure Q with the physical measure P using the following Radon–Nikodym derivative:

$$\frac{dQ}{dP} = \exp(-\int_0^t \epsilon_{1,s}dW_{2,s}^P - \int_0^t \epsilon_{2,s}d\bar{W}_{2,s}^P - \int_0^t \epsilon_{3,s}dW_{4,s}^P - \int_0^t \epsilon_{4,s}d\bar{W}_{4,s}^P - \frac{1}{2}\int_0^t \epsilon_{1,s}^2 ds - \frac{1}{2}\int_0^t \epsilon_{2,s}^2 ds - \frac{1}{2}\int_0^t \epsilon_{3,s}^2 ds - \frac{1}{2}\int_0^t \epsilon_{4,s}^2 ds),$$

Therefore, under Q, we have

$$W_{2,t}^Q = W_{2,t}^P + \int_0^t \epsilon_{1,s}ds,\ \bar{W}_{2,t}^Q = \bar{W}_{2,t}^P + \int_0^t \epsilon_{2,s}ds,$$
$$W_{4,t}^Q = W_{4,t}^P + \int_0^t \epsilon_{3,s}ds,\ \bar{W}_{4,t}^Q = \bar{W}_{4,t}^P + \int_0^t \epsilon_{4,s}ds,$$

With the above measure transformation, we have

$$dy_t = [\kappa_y(\theta_t - y_t) - \sigma_y e^{\psi(t)}\epsilon_{1,t}]dt + \sigma_y e^{\psi(t)}dW_{2,t}^Q,$$
$$dl_t = [\alpha(\beta - l_t) - \eta\epsilon_{3,t}]dt + \eta dW_{4,t}^Q.$$

One can clearly observe that the drift terms of the aforementioned processes have been modified as a result of the measure transformation. The supplementary terms, namely $\sigma_y e^{\psi(t)}\epsilon_{1,t}$ and $\eta\epsilon_{3,t}$ are identified as the market prices of risks associated with convenience yield and liquidity factors, respectively. Given the considerations of economic reasonableness and analytical tractability, market prices of risks are usually assumed to be a linear function of the corresponding source variable (Feng et al., 2014; He et al., 2025c). Consequently, we assume that

$$\sigma_y e^{\psi(t)}\epsilon_{1,t} = \gamma_1 y_t,\ \eta\epsilon_{3,t} = \gamma_2 l_t.$$

Denoting

$$\tilde{\kappa_y} = \kappa_y + \gamma_1,\ \tilde{\theta}_t = \frac{\kappa_y\theta_t}{\kappa_y + \gamma_1},$$
$$\tilde{\alpha} = \alpha + \gamma_2,\ \tilde{\beta} = \frac{\alpha\beta}{\alpha + \gamma_2},$$

we have

$$dy_t = \tilde{\kappa_y}(\tilde{\theta}_t - y_t)dt + \sigma_y e^{\psi(t)}dW_{2,t}^Q,$$
$$dl_t = \tilde{\alpha}(\tilde{\beta} - l_t)dt + \eta dW_{4,t}^Q,$$

The measure transform remains incomplete at this stage, as the commodity price, when discounted at the risk-free interest rate, must be a martingale in a risk-neutral world. It is therefore necessary to choose suitable values for $\epsilon_{2,t}$ and $\epsilon_{4,t}$ to ensure that the following identity holds:

$$\mu + \xi l_t + \frac{1}{2}\xi^2 l_t^2 - \frac{\sigma_1\rho_{zy}\gamma_1 y_t}{\sigma_y e^{\psi(t)}} - \frac{\xi\rho_{\zeta l}\gamma_2 l_t^2}{\eta} - \sqrt{1-\rho_{zy}^2}\sigma_1\epsilon_{2,t} - \sqrt{1-\rho_{\zeta l}^2}\xi l_t\epsilon_{4,t} = r.$$

Now, dropping all the tildes, we have the following price dynamics under the risk-neutral measure Q:

$$\frac{dS_t}{S_t} = (r - y_t)dt + \sigma_1\sqrt{y_t}dW_{1,t}^Q + \xi l_t dW_{3,t}^Q,$$
$$dy_t = \kappa_y[\theta(t) - y_t]dt + \sigma_y e^{\psi(t)}dW_{2,t}^Q,$$
$$dl_t = \alpha(\beta - l_t)dt + \eta dW_{4,t}^Q, \tag{3.1}$$

where $W_{1,t}^Q = \rho_{zy}W_{2,t}^Q + \sqrt{1-\rho_{zy}^2}\bar{W}_{2,t}^Q$, and $W_{3,t}^Q = \rho_{\zeta l}W_{4,t}^Q + \sqrt{1-\rho_{\zeta l}^2}\bar{W}_{4,t}^Q$. Note that $W_{2,t}^Q$, $\bar{W}_{2,t}^Q$, $W_{4,t}^Q$, and $\bar{W}_{4,t}^Q$ are independent with each other.

After establishing the price dynamics under the risk-neutral measure, the valuation of commodity futures options can be addressed, as will be detailed in the following two subsections.

3.2. Analytical price of futures

We first consider the determination of the commodity futures price $F(t;T)$, where T represents its maturity time. To facilitate the solution procedure, the following new variables and notations are adopted:

$$z_t = \ln S_t,\ Y_t = [z_t, y_t, l_t]^T,\ \tau = T - t,\ \phi = [\phi_1, \phi_2, \phi_3]^T,$$
$$D(\tau;\phi) = [D_1(\tau;\phi), D_2(\tau;\phi), D_3(\tau;\phi)]^T,$$

where $[\cdot]^T$ represents the transpose operation of a given matrix.

Since the futures price can be expressed as

$$F(t;T) = E^Q[S_T|g(t)] = E^Q[e^{z_t}|g(t)] = E^Q[e^{\tilde{\phi}Y_T}|g(t)],$$

where $\tilde{\phi} = [1, 0, 0]^T$, we derive $m(\phi, Y_t, t; T) = E^Q[e^{\phi Y_T}|g(t)]$ first, which represents the moment generating function of Y_T with the information of the full filtration g up to t already known. The futures price $F(t;T)$ can then be obtained through $F(t;T) = m(\tilde{\phi}, Y_t, t; T)$.

Since the stochastic process (3.1) is affine, one can assume that $m(\phi, Y_t, t; T)$ has an exponentially affine structure (He and Lin, 2024a,b) as

$$m(\phi, Y_t, t; T) = e^{C(\tau;\phi) + D(\tau;\phi)Y_t + D_4(\tau;\phi)l_t^2},$$

where $C(\tau;\phi)$ and $D(\tau;\phi)$ are unknown scalar and vector functions, respectively.

According to the Feynman–Kac formula, it is known that $m(\phi, Y_t, t; T)$ satisfies the following partial differential equation (PDE)

$$\frac{\partial m}{\partial t} + (r - y - \frac{\sigma^2}{2} - \frac{\xi^2 l^2}{2})\frac{\partial m}{\partial z} + \kappa_y(\theta_t - y)\frac{\partial m}{\partial y} + \alpha(\beta - l)\frac{\partial m}{\partial l} + \frac{1}{2}(\sigma_1^2 + \xi^2 l^2)\frac{\partial^2 m}{\partial z^2} + \frac{1}{2}\sigma_y^2 e^{2\psi(t)}\frac{\partial^2 m}{\partial y^2} + \frac{1}{2}\eta^2\frac{\partial^2 m}{\partial l^2} + \rho_{zy}\sigma_1\sigma_y e^{\psi(t)}\frac{\partial^2 m}{\partial z\partial y} + \rho_{\zeta l}\xi\eta l\frac{\partial^2 m}{\partial z\partial l} = 0$$

With lengthy derivatives, D_1, D_2, D_3 and D_4 can be solved as

$$D_1(\tau;\phi) = \phi_1,\ D_2(\tau;\phi) = (\frac{\phi_1}{\kappa_y} + \phi_2)e^{-\kappa_y\tau} - \frac{\phi_1}{\kappa_y},$$
$$D_3(\tau;\phi) = \frac{1}{A\sinh(m\tau) + \cosh(m\tau)}[\frac{8\alpha\beta c}{d^2}(\cosh(m\tau) - 1) + \phi_3],$$
$$D_4(\tau;\phi) = \frac{(d-b)(1-e^{d\tau})}{2a(1-ge^{d\tau})} = -\frac{b}{2a}\tau - \frac{1}{a}\ln[\cosh(m\tau) + A\sinh(m\tau)],$$

where

$$a = 2\eta^2,\ b = 2(\rho_{\zeta l}\xi\eta\phi_1 - \alpha),\ c = \frac{1}{2}\xi^2(\phi_1^2 - \phi_1),\ d = \sqrt{b^2 - 4ac},$$
$$g = \frac{b-d}{b+d},\ m = \frac{d}{2},\ A = -\frac{b}{d}.$$

Consequently, we have

$$C(\tau;\phi) = (r - \frac{\sigma_1^2}{2})\phi_1\tau + \frac{1}{2}\sigma_1^2\phi_1^2\tau + \kappa_y J_1 + \eta^2 J_2 + \frac{\eta^2}{2}J_3 + \frac{1}{2}\sigma_y^2 J_4 + \rho_{zy}\sigma_1\sigma_y\phi_1 J_5,$$

where

$$J_1 = \int_0^\tau \theta_t D_2(s;\phi)ds = \frac{\theta_0(\phi_1 + \phi_2\kappa_y)}{\kappa_y}(1 - e^{-\kappa_y\tau}) + \sum_{n=1}^N \frac{\phi_1 + \phi_2\kappa_y}{\kappa_y^2 + 4n^2\pi^2}(\kappa_y\gamma_n - 2\pi n\gamma_n^*)(\cos AT - e^{-\kappa_y\tau}\cos At) - \phi_1\theta_0\tau - \phi_1\sum_{n=1}^N \frac{\gamma_n[\sin 2\pi nT - \sin 2\pi n\tau] + \gamma_n^*[\cos 2\pi nt - \cos 2\pi nT]}{2\pi n}$$

$$J_2 = \int_0^\tau D_4(s;\phi)ds = -\frac{b}{2a}\tau - \frac{1}{a}\ln(\cosh(m\tau) + A\sinh(m\tau))$$
$$J_3 = \int_0^\tau D_3^2(s;\phi) + \frac{2\alpha\beta}{\eta^2}D_3(s;\phi)ds = \frac{\eta^2}{2}\frac{4\alpha^2\beta^2}{a^2}(① + ② + ③) - \frac{\alpha^2\beta^2}{2\eta^2}\tau,$$
$$J_4 = \int_0^\tau e^{2\psi(T-s)}D_2^2(s;\phi)ds,\ J_5 = \int_0^\tau e^{\psi(T-s)}D_2(s;\phi),$$

with

$$① = \frac{A^2}{m}[A + m\tau - \frac{\sinh(m\tau) + A\cosh(m\tau)}{A\sinh(m\tau) + \cosh(m\tau)}],$$
$$② = \frac{2A}{m}[1 - \frac{1}{A\sinh(m\tau) + \cosh(m\tau)}],$$
$$③ = \frac{(1-A^2)^2}{Am}\frac{1 - \cosh(m\tau)}{A\sinh(m\tau) + \cosh(m\tau)}.$$

For futures price, we have

$$F(t;T) = m(\tilde{\phi}, z, y, l) = e^{C(\tau;\tilde{\phi}) + z + D_2(\tau;\tilde{\phi})y}, \tag{3.2}$$

where $\tilde{\phi} = [1, 0, 0]$. From (3.2), it is clear that seasonality influences futures prices in both price and volatility levels, because both $\theta(t)$ and $\psi(t)$ are involved in this formula. However, liquidity is not included, suggesting that liquidity risks cannot be fully hedged by trading futures contracts alone. This is not surprising, because liquidity risks affect the commodity price through its volatility (Feng et al., 2014), but the changing in unspanned volatility will not affect the futures price (Trolle and Schwartz, 2009).

3.3. Analytical price of futures options

With the expression of $F(t;T)$ derived in the last subsection, we have

$$\frac{dF}{F} = \sigma_1 dW_{1,t}^Q + \xi l_t dW_{3,t}^Q + D_2(\tau;\tilde{\phi})\sigma_y e^{\psi(t)}dW_{2,t}^Q = \sigma_F dW_t^*,$$

where σ_F refers to the volatility of the underlying futures, and $\sigma_F^2 = \sigma_1^2 + \xi^2 l^2 + D_2^2\sigma_y^2 e^{2\psi(t)} + 2\rho_{zy}\sigma_1\sigma_y D_2(\tau;\tilde{\phi})e^{\psi(t)}$. From its expression, it is clear that σ_F relies on the state variable l_t, the variance terms of both S_t and y_t, the correlation between S_t and y_t, the speed of adjustment of y_t, and the time to maturity of the futures contract, but is independent of the state variables S_t and y_t. Therefore, to further solve for the price of options written on F, the following SDEs need to be used:

$$d\Theta(t;T) = -\frac{\sigma_F^2}{2}dt + \sigma_F dW_t^*,$$
$$dl_t = \alpha(\beta - l_t)dt + \eta dW_4,$$

where $\Theta(t;T) = \ln F(t;T)$ and $\mathrm{cov}(dW_t^*, dW_{4,t}^Q) = \rho_{\zeta l}dt$. Denote the moment generation function of $\Theta(t;T^*)$ as $\Phi(u,\Theta,l,t;T,T^*)$. According to the Feynman–Kac formula, we have

$$\frac{\partial\Phi}{\partial t} - \frac{\sigma_F^2}{2}\frac{\partial\Phi}{\partial\Theta} + \alpha(\beta - l)\frac{\partial\Phi}{\partial l} + \frac{\sigma_F^2}{2}\frac{\partial^2\Phi}{\partial\Theta^2} + \frac{\eta^2}{2}\frac{\partial^2\Phi}{\partial l^2} + \rho_{\zeta l}\xi l\eta\frac{\partial^2\Phi}{\partial\Theta\partial l} = 0.$$

We further assume that $\Phi(u,\Theta,l,t;T,T^*)$ has an exponentially affine structure as

$$\Phi(u,\Theta,l,t;T,T^*) = e^{h(\tau;u) + h_1(\tau;u)\Theta_t + h_2(\tau;u)l + h_3(\tau;u)l^2}.$$

Consequently, by solving the above PDE, we have

$$h_1(\tau;u) = u,$$
$$h_2(\tau;u) = \frac{2\alpha\beta}{a}[\frac{A\sinh(m\tau) + A^2\cosh(m\tau) + 1 - A}{\cosh(m\tau) + A\sinh(m\tau)} - 1],$$
$$h_3(\tau;u) = -\frac{b}{2a}\tau - \frac{1}{a}\ln(\cosh(m\tau) + A\sinh(m\tau)),$$

where $a = 2\eta^2$, $b = 2(\rho_{\zeta l}\xi\eta u - \alpha)$, $c = \frac{1}{2}\xi^2(u^2 - u)$, $d = \sqrt{b^2 - 4ac}$, $g = \frac{b-d}{b+d}$, $m = \frac{d}{2}$, $A = -\frac{b}{d}$. With h_1, h_2 and h_3 available, $h(\tau;\phi)$ can be derived as

$$h(\tau;u) = \frac{1}{2}(u^2 - u)\sigma_1^2\tau + \frac{1}{2}(u^2 - u)\sigma_y^2\int_0^\tau D_2(s + \tau_1;\tilde{\phi})e^{2\psi(T-s)}ds$$
$$+ (u^2 - u)\rho_{zy}\sigma_1\sigma_y\int_0^\tau D_2(s + \tau_1;\tilde{\phi})e^{\psi(T-s)}ds$$
$$- b\tau - \frac{1}{2}\ln(\cosh(m\tau) + A\sinh(m\tau)) + \frac{\eta^2}{2}\frac{4\alpha^2\beta^2}{a^2}(① + ② + ③) - \frac{\alpha^2\beta^2}{2\eta^2}\tau.$$

where

$$① = \frac{A^2}{m}[A + m\tau - \frac{\sinh(m\tau) + A\cosh(m\tau)}{A\sinh(m\tau) + \cosh(m\tau)}],$$
$$② = \frac{2A}{m}[1 - \frac{1}{A\sinh(m\tau) + \cosh(m\tau)}],$$
$$③ = \frac{(1-A^2)^2}{Am}\frac{1 - \cosh(m\tau)}{A\sinh(m\tau) + \cosh(m\tau)}.$$

With the expression of $\Phi(u,\Theta,l,t;T,T^*)$, the price of a European call option written on $F(t;T^*)$ can finally be written as

$$C(S,y,l,t;T,T^*) = \frac{1}{2}e^{-r(T-t)}\Phi(1,\ln F(t;T^*),y,l,t;T,T^*)$$
$$+ \frac{e^{-r(T-t)}}{\pi}\int_0^\infty \Re[\frac{e^{-iu\ln K}\Phi(iu+1,\ln F(t;T^*),l,t;T,T^*)}{iu}]du$$
$$- Ke^{-r(T-t)}\{\frac{1}{2}$$
$$+ \frac{1}{\pi}\int_0^\infty \Re[\frac{e^{-iu\ln K}\Phi(iu,\ln F(t;T^*),l,t;T,T^*)}{iu}]du\}. \tag{3.3}$$

The put price can be obtained in a similar manner. For simplicity, we omit the details here.

From the expression of the option pricing formula, two remarks should be made before leaving this section. Firstly, liquidity risks have an impact on the option price through the volatility of the underlying futures, rather than the futures price itself. Secondly, given the corresponding futures price, the price level seasonality, i.e., $\theta(t)$, does not appear in the option pricing formula, indicating that it has no effect on the option price. This agrees with the empirical findings given by Back et al. (2013).

So far, we have derived a semi-closed-form analytical pricing formula for European commodity futures options, incorporating seasonality and liquidity risks. This formula will be validated by comparing with the MC simulation results, which will be presented in the subsequent section. The analytical solution facilitates quantitative evaluations of the impact of seasonality and liquidity risks on the pricing of futures options, which will also be the main emphasis of the subsequent section.

4. Numerical examples and discussions

This section examines the numerical validation of the newly derived formula and investigates the impact of seasonality and liquidity risks on the pricing of European futures options. In the subsequent numerical experiments, unless specified otherwise, the following parameters are adopted: $r = 0.06$, $K = 500$, $S_0 = 500$, $t = 0$, $T = 0.5$, $T^* = 1$, $\sigma_1 = 0.162$, $\sigma_y = 0.347$, $\xi = 0.6$, $\kappa_y = 1.988$, $y_0 = 0.1919$, $l_0 = 0.0909$, $\theta_0 = -0.0542$, $N = 2$, $\gamma_1 = 0.025$, $\gamma_2 = -0.01$, $\gamma_1^* = -0.126$, $\gamma_2^* = 0.028$, $q = 0.1612$, $\upsilon = -0.0069$, $\alpha = 3$, $\beta = 0.3$, $\eta = 0.2$, $\rho_{\zeta l} = -0.2$, $\rho_{zy} = 0.3$. All numerical experiments are done on a PC with Intel(R) Core(TM) i5-1340P CPU@1.90 GHz 4.60 GHz and 18.30 GB of RAM.

4.1. Validity and efficiency

The validity of the newly derived formula will be checked by comparing the analytical option prices with those obtained by the MC simulations. It is important to note that the traditional MC approach exhibits inefficiency in pricing futures options. The total number of routes used to simulate the option price at a specific point (S_t, y_t, l_t) is the product of the routes used in $(t,T]$ for simulating the expected value of the payoff and those used in $(T,T^*]$ for simulating one futures price at T. The traditional MC approach requires more than one day to produce the option price at a single point using 2×10^5 routes in both periods.

In view of this, a modified MC approach is adopted in the current study. The MC is firstly applied to (3.1) to generate possible values of S_T, y_T, and l_T. With S_T, y_T and l_T available, $F(T;T^*)$ is then calculated

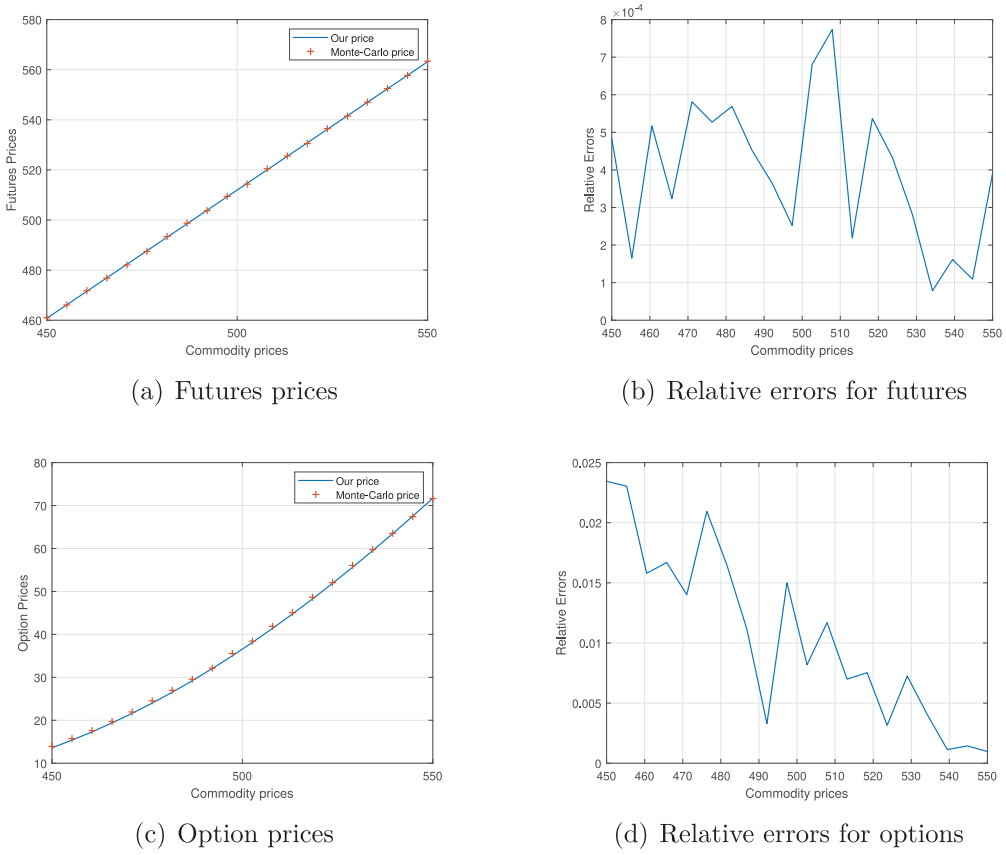

(a) Futures prices (b) Relative errors for futures

(c) Option prices (d) Relative errors for options

Fig. 1. MC prices VS analytical prices.

through (3.2). The commodity futures option price is finally determined through

$$C_{MC}(S, y, l, t; T; T^*) = \frac{e^{-r(T-t)}}{N} \sum_{j=1}^{N} \max[F_j(T; T^*) - K, 0],$$

where N is the number of routes used in the MC simulation.

Depicted in Fig. 1 are the comparisons of the analytical and MC futures and futures option prices. From Fig. 1(a), one can clearly observe that the two prices agree well with each other, with the maximum on-dot relative error across being less than 0.08%, as suggested in Fig. 1(b). With the validity of the analytical futures price in hand, the prices of the futures options are then simulated and compared, as shown in Fig. 1(c). This figure also illustrates a strong agreement between the analytical futures option prices and the corresponding MC results. The maximum on-dot relative error between the two is less than 2.5%, as further shown in Fig. 1(d). This validates both the formulas and their implementation techniques.

Remarkably, while the modified MC method shows a notable decrease in computational time, the current method exhibits an even more significant reduction. In specific, the current formula requires 0.0732 s to generate a single futures price and 4.2070 s for an option price, while the MC method with 2×10^5 routes requires 1.5090 s and 46.7895 s for the corresponding tasks. This indicates that a time reduction of over 90% can be achieved once the analytical formulas are adopted, in comparison to the MC method.

With confidence in the current solution, in the following, we shall examine the influences of seasonality and market liquidity on the price of European calls issued on commodity futures.

4.2. Sensitivity analysis

The price of a European futures call option is firstly computed using varying parameters of liquidity risks to assess their impacts. Fig. 2(a) shows that the option price is monotonically increasing w.r.t ξ. Intuitively, as the return of the commodity price becomes more sensitive to the level of market illiquidity, the uncertainty about future commodity price increases, resulting in higher option prices. Figs. 2(b) and 2(c) demonstrate a similar trend when the mean-reversion rate or absolute value of the long-term mean rises. This is because an increase in either α or $|\beta|$ would result in a larger "averaged" market illiquidity level, which warrants higher option price to compensate for the resultant high liquidity risks. The sensitivity of commodity futures option price w.r.t the volatility of the market illiquidity is presented in Fig. 2(d). Unsurprisingly, the volatility of illiquidity and the option price are positively correlated. One possible explanation is that the uncertainty of the illiquidity raises the expectation of the volatility of the commodity price returns so that the party who holds a long position in the commodity futures should be compensated.

On the other hand, as mentioned in Back et al. (2013) and Ma et al. (2020), the volatility of commodity futures demonstrates strong seasonal patterns, which further influences the prices of futures and options. In the following, we shall investigate how key seasonal parameters influences the volatility of futures.

Fig. 3(a) demonstrates a nonlinear relationship between q and the volatility of futures price. From this figure, it is clear that q controls the amplitude of volatility clustering, with higher values leading to more pronounced cyclical peaks, implying that q might arise from fundamental drivers like production cycles and demand variations. Importantly, a threshold effect can also be observed from this figure, which suggest that beyond certain critical levels, small increases in q

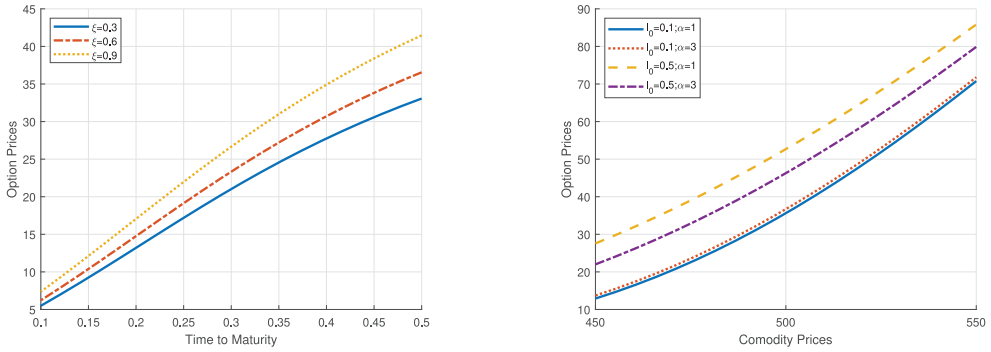

(a) The effect of ξ (b) The effect of α

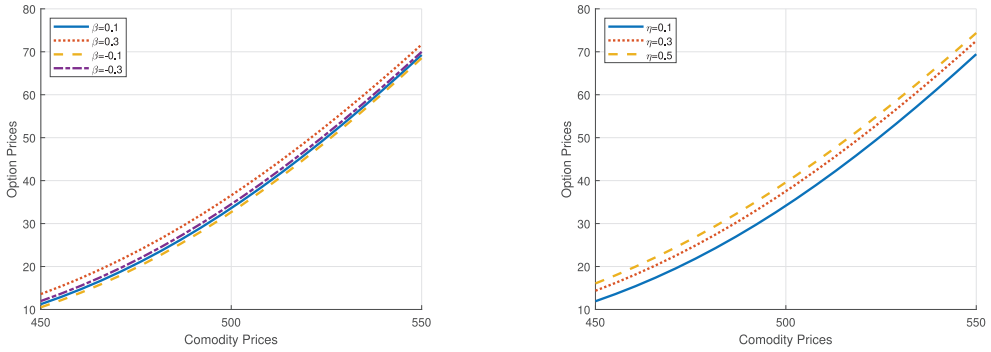

(c) The effect of β (d) The effect of η

Fig. 2. Impacts of key parameters of liquidity risks.

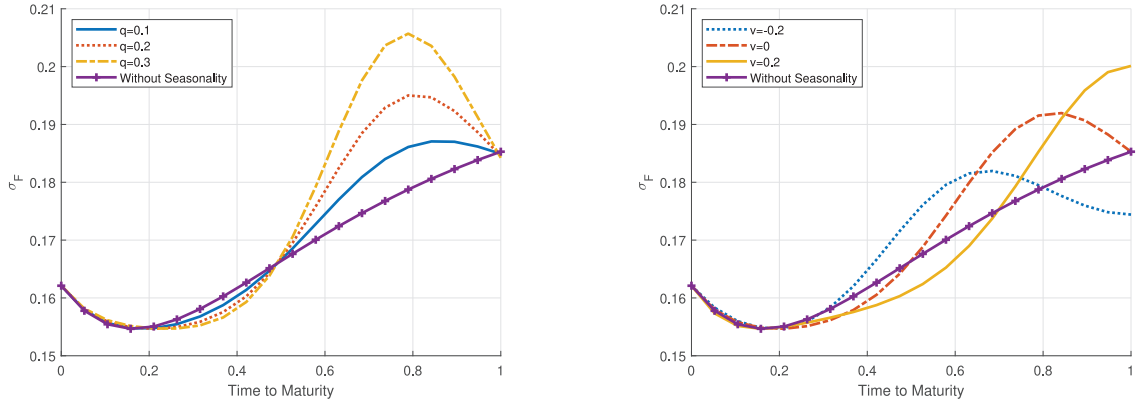

(a) (b)

Fig. 3. The effects of q and v on futures volatility.

generate disproportionately large volatility spikes, indicating potential regime shifts in market behavior during extreme seasonal conditions.

Fig. 3(b) investigates the impact of parameter v on the futures volatility. Unlike q which affects the amplitude, v translates the entire seasonal cycle along the time axis without distorting its shape. The figure reveals that v operates as a timing regulator with higher values systematically delaying peak volatility periods and lower values advancing them. This linear phase-response characteristic suggests that v likely captures institutional or operational delays in market adjustments, such as storage replenishment lags or transportation bottlenecks.

5. An empirical study

This section provides an empirical study to assess the pricing performance of the current model in comparison to the basic and CS models. The data set and various filters are presented initially, succeeded by a detailed explanation of the model calibration process. The empirical findings are finally presented and analyzed. Beyond investigating option pricing performance, we extend the empirical analysis to underlying futures contracts, a critical examination given the theoretical requirement for consistent pricing across derivatives and their underlyings within a unified framework.

5.1. Data description

The data set for our empirical investigation comprises of daily commodity futures option prices and related futures contracts issued on the Shanghai INE Crude Oil. All data were taken from Shanghai International Energy Exchange (https://www.ine.cn/). Our sampling period covers a whole year from January 2024 to January 2025, allowing us to capture seasonal patterns in option and futures pricing across 12 calendar months. It should be pointed out that using Shanghai INE crude oil futures and options data to test the proposed pricing model incorporating both liquidity risk and seasonal effects is theoretically justified. The INE market's distinct seasonal patterns driven by China's cyclical demand fluctuations and policy interventions, align well with the model's seasonal component, particularly when parameters like q and υ are properly calibrated to reflect observed volatility peaks. Meanwhile, the market's moderate liquidity compared to global benchmarks provides a suitable environment for evaluating the effects of liquidity risks.

It should be pointed out that the semi-closed form solution (3.3) is applicable to European-style options only. However, all options in our data set are American-style contracts. This involves the conversion of American option prices to their European counterparts, using a widely accepted method when only American options data is accessible in the financial market (Brignone et al., 2024; Trolle and Schwartz, 2009). We begin by determining the implied volatility through inverting the Barone-Adesi-Whaley (BAW) formula for each option, using the price available in the current financial market (Barone-Adesi and Whaley, 1987). We then use the implied volatility and the Black formula to calculate the European option price, which serves as the market price to match the model price generated from the current formula with market-based characteristics.

In the following work, no filters are applied to the futures, and models are estimated using all observations from one week. However, it is essential to remove sample noise from the raw data set to prevent misleading outcomes in pricing options. To deal with the "day-of-the-week" effect, option prices from Wednesday and Thursday are selected. Specifically, prices on Wednesday are utilized to estimate parameters, which then serve as model parameters for predicting call prices on Thursday (Bakshi et al., 1997; He et al., 2025a). To mitigate the effects of inaccuracies in the early exercise approximation using the BAW formula, we choose options with absolute moneyness in the range $[0.9, 1.1]$ (Trolle and Schwartz, 2009). Here, the absolute moneyness is defined as the absolute difference between the underlying futures price and the strike price, divided by the strike price. It should also be noted that the risk-free interest rate is proxied by the daily published 3-month SHIBOR rate, as the expiry time of the options and futures contracts is less than 3 months.

After all these filters being applied, it is ready to move on to the parameter estimation step, which is discussed in the next subsection.

5.2. Model estimation

While contract characteristics such as maturity and strike price of the options are predetermined, and the price of the commodity along with the risk-free rate is observable, the model parameters are not. They need to be estimated from market data. We now specify the models' parameters before estimating them.

Denote the sets of parameters need to be determined as Ψ_{basic}, Ψ_{CS} and Ψ_{CSL} for the basic model, the CS model and the CSL model, respectively. The parameters need to be estimated for each model are:

$$\begin{aligned}\Psi_{basic} &= \{r, \sigma_1, \rho_{zy}, \kappa_y, \theta_0, \sigma_y, y_0\},\\ \Psi_{CS} &= \{r, \sigma_1, \rho_{zy}, \kappa_y, \theta_0, \gamma_1, \gamma_2, \gamma_1^*, \gamma_2^*, q, \upsilon, \sigma_y, y_0\},\\ \Psi_{CSL} &= \{r, \sigma_1, \rho_{zy}, \kappa_y, \theta_0, \gamma_1, \gamma_2, \gamma_1^*, \gamma_2^*, q, \upsilon, \sigma_y, \xi, \alpha, \beta, \eta, \rho_{\zeta l}, y_0, l_0\}.\end{aligned}$$

Table 1
Estimated parameters for the three models from futures options.

	The basic model	The CS model	The CSL model
σ_1	0.3140	0.3313	0.3105
ρ_{zy}	0.2909	0.4964	0.4818
κ_y	4.5540	3.7941	5.8582
q	–	2.6335	2.6582
υ	–	−0.1421	−0.2044
σ_y	1.0558	2.2365	2.3840
ξ	–	–	0.1259
α	–	–	5.7151
β	–	–	−0.1190
η	–	–	1.6839
$\rho_{\zeta l}$	–	–	0.1521
l_0	–	–	0.0274

Table 2
Estimated parameters associated with the long-term mean from futures.

	θ_0	γ_1	γ_2	γ_1^*	γ_2^*
the basic model	0.1691	–	–	–	–
the CS/CSL model	0.2055	0.0302	−0.0448	0.0356	0.0290

Parameters are estimated through the numerical minimization of a loss function that quantifies the pricing discrepancies between theoretical model prices and observed market prices. In accordance with established literature (Lim and Zhi, 2002), the mean squared error (MSE) is employed as the objective function. The MSE is defined as

$$\text{MSE} = \frac{1}{N}\sum_{i}^{N}(V_i^{market} - V_i^{model})^2, \tag{5.1}$$

where V_i^{market} represents the market price and V_i^{model} denotes the corresponding model price for the ith observation, with N indicating the number of observations in a single estimation.

A further examination of the goal function (5.1) indicates that it may not be convex, potentially resulting in multiple local minima. Therefore, in this study, a global optimization approach is adopted instead of any local minimization strategy to prevent the occurrence of local minima and to achieve the global minimum effectively. The integrated genetic algorithm within Matlab is employed to solve the minimization problem. The estimated daily-averaged parameters for the three models are presented in Tables 1 and 2. We remark that in the context of options, the long-term mean $\theta(t)$ does not enter the pricing formula, and thus parameters associated with $\theta(t)$, specifically $\{\theta_0, \gamma_1, \gamma_2, \gamma_1^*, \gamma_2^*\}$, are estimated independently from the underlying futures. In addition, since liquidity risks do not affect the futures prices, these parameters (i.e., $\{\theta_0, \gamma_1, \gamma_2, \gamma_1^*, \gamma_2^*\}$) are the same under both the CS and CSL models.

It should be remarked that the calibration results shown in Table 1 are well-supported by the fundamental behavior of China's INE crude oil market during the Year 2024 to 2025. The parameters associated with liquidity risks reveal a market with meaningful but transient liquidity pressures. Specifically, the high mean-reversion rate ($\alpha = 5.7151$) appropriately captures the rapid adjustment characteristic of China's policy-responsive financial environment, while the liquidity volatility ($\eta = 1.6939$) indicates more pronounced liquidity risk fluctuations compared to typical emerging markets, which reasonably reflects the INE market's evolving microstructure and occasional liquidity stresses. The negative long-term mean ($\beta = -0.1190$) reasonably reflects the liquidity premium inherent in China's INE crude oil market due to capital controls and participation constraints.

Regarding seasonal factors, the model successfully incorporates China's unique demand patterns. The significant amplitude ($q = 2.6582$) accurately reflects pronounced cyclical fluctuations driven by China-specific demand patterns, including Spring Festival inventory builds and post-holiday industrial recovery. The phase shift parameter ($\upsilon =$

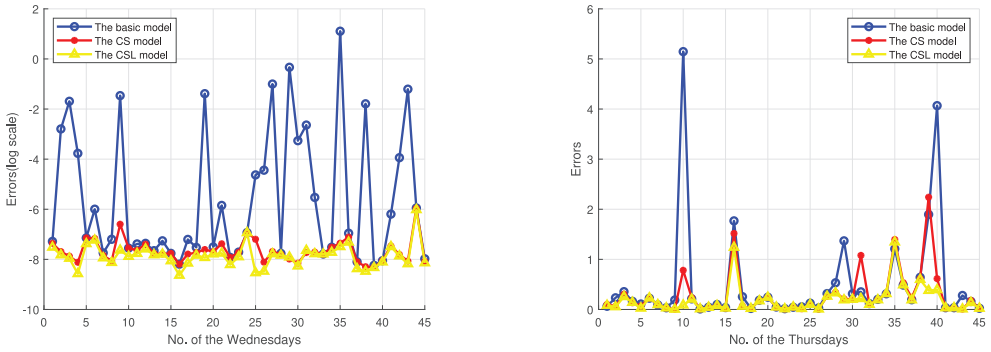

(a) Weekly in-sample-errors (b) Weekly out-of-sample-errors

Fig. 4. Comparisons of the weekly errors.

Table 3
Errors of the three models for pricing futures.

	In-sample MSE	Out-of-sample MSE
The basic model	12.0940	44.6814
The CS/CSL model	6.7804	40.1300

Table 4
Errors of the three models for pricing futures options.

	In-sample MSE	Out-of-sample MSE
The basic model	0.1223	0.4967
The CS model	0.0005	0.2907
The CSL model	0.0004	0.1935

−0.2044) properly accounts for the earlier timing of seasonal peaks in China's market compared to global benchmarks, aligning with Chinese economic activity cycles. The elevated long-term mean ($\theta_0 = 0.2055$) appropriately represents China's convenience yield premium as the world's largest crude oil importer, while seasonal coefficients ($\gamma_1 = 0.0302$, $\gamma_1^* = 0.0356$) characterize the unique bimodal seasonality of post-Spring Festival demand and autumn consumption peaks. The model further incorporates policy-induced quarterly variations through parameters like $\gamma_2 = -0.0448$, effectively mirroring strategic reserve rotation patterns.

All together, these carefully estimated parameters indeed provide a comprehensive framework for understanding China's INE's price formation mechanisms, though minor adjustments might be needed to account for evolving energy transition trends and geopolitical influences.

5.3. Model performance

This subsection compares the pricing performance of the CSL model to the basic model and the CS model with parameters estimated from the actual financial market. Pricing performance is evaluated with both in- and out-of-sample errors. While the former refers to the difference between market and model prices during the model calibration stage, the latter is the "prediction" error calculated using market prices from a separate data set that was not employed for model calibration, as well as model prices computed with parameters estimated during the model calibration stage.

The errors for the three models in terms of pricing futures are shown in Table 3. From this table, it is clear that the basic model shows the highest errors, while both the CS and CSL models demonstrate identical improved accuracy. The identical MSE values for CS and CSL models confirm that liquidity factors, while included in CSL, do not affect futures pricing. Seasonal factors contribute to the pricing performance for futures by deducing the in- and out-of sample errors by 43.49% and 10.19%, respectively. Note that the absolute MSE magnitudes appear large because futures prices themselves typically have high values (e.g., energy or metal contracts often trade in hundreds of dollars).

The errors of the three models in terms of pricing options are presented in Table 4. The results demonstrate the superior pring performance of the CSL model for energy derivatives, where seasonal effects and liquidity risks play a critical role. Specifically, the CSL model reduces the in-sample error to 0.0004, a 99.7% improvement over the basic model's error of 0.1223. More importantly, its out-of-sample error shows a 61% reduction compared to the basic model, underscoring its robustness in practical applications. The advantages of incorporating seasonal factors are obvious when comparing the CS model with the basic model: the CS model achieves a 99.6% reduction in in-sample error and a 41.6% improvement in out-of-sample accuracy. Furthermore, the incremental benefit of adding liquidity adjustments becomes clear when comparing the CSL model to the CS model. The CSL model delivers a 33.5% improvement in out-of-sample performance, emphasizing the importance of liquidity risk factors alongside seasonal adjustments. This enhancement is particularly valuable in energy markets, where trading volumes and market depth exhibit significant fluctuations. A deeper inspection of the weekly in-sample and out-of-sample errors, as shown in Fig. 4, implies that the current model outperforms the other two in almost every week during the sampling period. One should notice that the basic model's larger in-sample dataset compresses some curves near the bottom axis. As a result, we use logarithmic scaling on the vertical axis for clearer visualization, as shown in Fig. 4(a).

Another issue of common interest is how well the model performs across different moneyness. Table 5 presents out-of-sample pricing errors across three moneyness categories, classified by the underlying futures-to-strike price ratio (F/K) as out-of-the-money (OTM, $F/K < 0.97$), at-the-money (ATM, $0.97 \leq F/K \leq 1.03$), and in-the-money (ITM, $F/K > 1.03$). The superior accuracy of the CSL model is most pronounced for ATM options, where it achieves a 58.5% error reduction compared to the basic model and a further 23.2% improvement over the CS model. The CS model's intermediate results reveal that while seasonal adjustments provide substantial benefits (47.3% improvement versus the basic model), the explanatory power of the liquidity risks is not significant for ITM options, where the CSL model offers only an additional 20.8% enhancement. All the three models exhibit particularly strong performance for OTM options, due to the use of the BAW formula (Schwartz and Smith, 2000). The CSL model maintains this advantage while further reducing the pricing errors in the OTM category by 61.1% and 48.2%, compared to the basic and CS models, respectively. These moneyness-dependent performance patterns suggest that while seasonality and liquidity factors are universally important, their relative contribution varies across the moneyness spectrum. The robust performance of the CSL model across all categories confirms

Table 5
Out-of-sample errors across different moneyness.

Moneyness	ATM	ITM	OTM
The basic model	0.3735	0.6751	0.4022
The CS model	0.2018	0.3558	0.2084
The CSL model	0.1550	0.2819	0.1565

again the importance of incorporating both seasonal and liquidity factors for pricing energy futures options.

6. Conclusion

This work provides an analytical solution for the pricing of European futures options under a newly proposed CSL model. The primary contributions of the current work may be condensed into three key elements: (i) It is the first in the literature that takes into account both the seasonality and liquidity risks. The proposed CSL model is shown empirically to be more suitable to the actual energy markets. (ii) A semi-closed-analytical formula for the price of futures options is successfully derived. This formula is easy to implement, and is proved numerically to be superior to the MC simulations in terms of pricing efficiency. (iii) An empirical study using options on crude oil futures is conducted. The empirical results show that the CSL model outperforms the basic model and the CS model, implying that the CSL model, along with the analytical formula, could be safely used in energy futures option market.

CRediT authorship contribution statement

Wenting Chen: Methodology, Formal analysis, Writing – review & editing, Software. **Zhao Yang:** Formal analysis, Writing – original draft, Investigation. **Xin-Jiang He:** Conceptualization, Writing – review & editing, Software, Investigation.

Acknowledgments

This work is supported by the Ministry of Education of Humanities and Social Science Project of China (No. 21YJAZH005), the National Natural Science Foundation of China (No. 12101554), the Fundamental Research Funds for Zhejiang Provincial Universities (No. GB202103001), and the Research Project of Zhejiang Federation of Humanities and Social Sciences, China (No. 2025N095).

Appendix A. Supplementary data

Supplementary material related to this article can be found online at https://doi.org/10.1016/j.eneco.2025.108737.

References

Back, J., Prokopczuk, M., Rudolf, M., 2013. Seasonality and the valuation of commodity options. J. Bank. Financ. 37 (2), 273–290.
Bakshi, G., Cao, C., Chen, Z., 1997. Empirical performance of alternative option pricing models. J. Financ. 52 (5), 2003–2049.
Barone-Adesi, G., Whaley, R., 1987. Efficient analytic approximation of American option values. J. Financ. 42, 301–320.
BIS, 2023. BIS quarterly review: December 2023. https://www.bis.org/publ/qtrpdf/r-qt2312.pdf.
Brignone, R., Gonzato, L., Sgarra, C., 2024. Commodity Asian option pricing and simulation in a 4-factor model with jump clusters. Ann. Oper. Res. 336 (1), 275–306.
Chen, S.-H., Chiou-Wei, S.-Z., Zhu, Z., 2022. Stochastic seasonality in commodity prices: the case of US natural gas. Empir. Econ. 62 (5), 2263–2284.
CME Group, 2023. 2023 annual report. https://www.cmegroup.com/annual-reports/2023-annual-report.pdf.
Constant, A., Marie-Hélène, G., Gabriel J, P., 2023. The performance of jump models to price commodity options. J. Deriv. 31 (2).
Ewald, C.-O., Haugom, E., Lien, G., Størdal, S., Wu, Y., 2022. Trading time seasonality in commodity futures: An opportunity for arbitrage in the natural gas and crude oil markets? Energy Econ. 115, 106324.
Ewald, C.-O., Ouyang, R., 2017. An analysis of the fish pool market in the context of seasonality and stochastic convenience yield. Mar. Resour. Econ. 32 (4), 431–449.
Feng, S.P., Huang, M.W., Wang, Y.H., 2014. Option pricing with stochastic liquidity risk: Theory and evidence. J. Financ. Mark. 18, 77–95.
Frau, C., Fanelli, V., 2024. Seasonality in commodity prices: New approaches for pricing plain vanilla options. Ann. Oprations Res. 336, 1089–1131.
Geman, H., 2005. Commodities and Commodity Derivatives: Modeling and Pricing for Agriculturals, Metals and Energy. John Wiley & Sons.
Gibson, R., Schwartz, E.S., 1990. Stochastic convenience yield and the pricing of oil contingent claims. J. Financ. 45, 959–976.
He, X.-J., Chen, H., Lin, S., 2025a. A closed-form formula for pricing European options with stochastic volatility, regime switching, and stochastic market liquidity. J. Futur. Mark. 45 (5), 429–440.
He, X.-J., Huang, S.-D., Lin, S., 2025b. A closed-form solution for pricing European-style options under the heston model with credit and liquidity risks. Commun. Nonlinear Sci. Numer. Simul. 143, 108595.
He, X.-J., Lin, S., 2024a. Analytical formulae for variance and volatility swaps with stochastic volatility, stochastic equilibrium level and regime switching. AIMS Math. 9 (8), 22225–22238.
He, X.-J., Lin, S., 2024b. Analytically pricing foreign exchange options under a three-factor stochastic volatility and interest rate model: A full correlation structure. Expert Syst. Appl. 246, 123203.
He, X.-J., Wei, W., Lin, S., 2025c. A closed-form formula for pricing exchange options with regime switching stochastic volatility and stochastic liquidity. Int. Rev. Financ. Anal. 103, 104159.
Hu, C.H., Li, Z.B., Liu, X.Y., 2020. Liquidity shocks, commodity financialization, and market comovents. J. Futur. Mark. 40, 1315–1336.
Jain, P.K., Kayhan, A., Onur, E., 2024. Determinants of commodity market liquidity. Financ. Rev. 59, 9–30.
Kalaitzoglou, I.A., Ibrahim, B.M., 2015. Liquidity and resolution of uncertainty in the European carbon futures market. Int. Rev. Financ. Anal. 37, 89–102.
Leippold, M., Schärer, S., 2017. Discrete-time option pricing with stochastic liquidity. J. Bank. Financ. 75, 1–16.
Li, Z., Zhang, W.G., Liu, Y.J., 2018. European quanto option pricing in presence of liquidity risk. North Am. J. Econ. Financ. 45, 230–244.
Lim, K.G., Zhi, D., 2002. Pricing options using implied trees: Evidence from FTSE-100 options. J. Futur. Mark. 22 (7), 601–626.
Lin, S., Chen, M., He, X.-J., 2025. Analytically pricing crude oil options under a jump-diffusion model with stochastic liquidity risk and convenience yield. North Am. J. Econ. Financ. 78, 102424.
Liu, H., Yong, J., 2005. Option pricing with an illquid underlying asset market. J. Econom. Dynam. Control 29, 2125–2156.
Loeper, G., 2018. Option pricing with linear market impact and nonlinear black-scholes equations. Ann. Appl. Probab. 28, 2664–2726.
Lucia, J.J., Schwartz, E.S., 2002. Electricity prices and power derivatives: Evidence from the Nordic power exchange. Rev. Deriv. Res. 5, 5–50.
Ma, Z., Ma, C., Wu, Z., 2020. Closed-form analytical solutions for options on agricultural futures with seasonality and stochastic convenience yield. Chaos Solitons Fractals 137, 109849.
Mellios, C., Six, P., Lai, A.N., 2016. Dynamic speculation and hedging in commodity futures markets with a stochastic convenience yield. European J. Oper. Res. 250 (2), 493–504.
Okoroafor, U.C., Leirvik, T., 2024. Dynamic link between liquidity and return in the crude oil market. Cogent Econ. Financ. 12, 2302636.
Pasricha, P., Zhu, S.P., He, X.J., 2022. A closed-form pricing formula for European options in an illiquid asset market. Financ. Innov. 8, 1–28.
Peng, K., Hu, Z.P., Rode, M.A., 2024. Maximum order size and market quality: Evidence from a natural experiment in commodity futures markets. J. Futur. Mark. 44, 803–825.
Schwartz, E.S., 1997. The stochastic behavior of commodity prices: Implications for valuation and hedging. J. Financ. 52 (3), 923–973.
Schwartz, E.S., Smith, J.E., 2000. Short term variations and long–term dynamics in commodity prices. Manag. Sci. 46, 893–911.
Trolle, A.B., Schwartz, E.S., 2009. Unspanned stochastic volatility and the pricing of commodity derivatives. Rev. Financ. Stud. 22 (11), 4423–4461.
Zhang, Y.M., Ding, S.S., 2018. Return and volatility co-movement in commodity futures markets: The effect of liquidity risks. Quant. Finance 18, 1471–1486.